JOURNAL OF GUIDANCE, CONTROL, AND DYNAMICS
Vol. 15, No. 2, March-April 1992

Parameter Sensitivity Reduction in Fixed-Order Dynamic Compensation

Anthony J. Calise* and Edward V. Byrns Jr.†
Georgia Institute of Technology, Atlanta, Georgia 30332

This paper presents a simple formulation for designing fixed-order dynamic compensators that are robust to uncertainty at the plant input and have reduced sensitivity to structured uncertainty in the plant dynamics. An approximate loop transfer recovery technique is extended to include a penalty on the trajectory sensitivity dynamics. This approach avoids introducing the sensitivity states, and thus the dimension of the optimization problem is not increased. The usefulness of the technique is illustrated by two compensator designs. The first design considers a case where the uncertain parameters occur in the output matrix. The second design is for a high bandwidth controller for a flexible spacecraft.

Introduction

RECENTLY, there has been a significant amount of research devoted to developing controllers that are robust to structured plant variations. There are two large classes of approaches: those that are norm bounding in the parameter uncertainty,[1-7] and those that attempt to reduce sensitivity to parameter uncertainty.[8-10] Whereas sensitivity reduction methods are limited in their ability to model the effects of finite (not infinitesimal) parameter uncertainty, the guarantees provided by perturbation bounding methods may come at a great sacrifice in performance or control effort. This is due to the fact that little is known about the conservativeness of the resulting bounds. In general, the utility of all of these approaches is highly problem dependent.

Norm-Bounding Methods

Several norm-bounding methods have been developed using a two-input/two-output (TITO) model to represent the uncertain system.[1-3] This representation uses an internal feedback loop to model the effect of parameter variations. In Refs. 1 and 2, TITO modeling is used in an H_∞ design formulation to guarantee stability in the presence of structured uncertainty. A similar approach is also taken in Ref. 3 using a game theoretic setting. Although these formulations are amenable to state space solution methods, they treat the effect of parameter perturbations as a complex and frequency-dependent uncertainty block, which may lead to a conservative design. The conservativeness inherent in these design approaches can be reduced by employing the μ-synthesis method.[4] This method optimizes the compensator design so that the μ measure,[5] or structured singular value, is minimized. The solution reduces to a parameter optimization problem using a so-called *D-K* iteration process that employs an H_∞ minimization as one of the iteration steps. Whereas μ synthesis allows multiple uncertainty blocks, conservatism remains since all uncertainty blocks permit complex variations. Although the real μ-analysis problem has been formulated, the real μ-synthesis problem remains a topic of current research.[6]

Sensitivity Reducing Methods

Sensitivity reducing methods rely on the addition of a quadratic penalty on the trajectory sensitivity to the standard linear-quadratic-Gaussian (LQG) formulation. The full state feedback formulation was first presented in Ref. 8, where the controller presupposes that the sensitivity states are available for feedback. This restriction was later removed by formulating an output feedback with full order observer design.[9] The difficulty that arises in sensitivity reduction is that the dimension of the problem (and consequently that of the controller) grows rapidly as the number of uncertain parameters increases. This problem was partially circumvented in Ref. 10 by fixing the order of the controller to that of the plant. Unfortunately, the dimension of the optimization problem is $2n(1+h)$, where n is the order of the plant and h is the number of uncertain parameters.

Fixed-Order Dynamic Compensation

Fixed-order dynamic compensator design was first introduced in 1970.[11] The major objections that emerged later were that the compensator formulation was overparameterized and that there were no guarantees on stability margins. Since that time a number of papers have appeared that have alleviated these objections in one form or another. In Ref. 12, the necessary conditions are obtained in the form of optimal projection equations. The projection operator removes the dependence of the solution on the controller parameterization, and the necessary conditions reduce to standard LQG Riccati equations when the order of the compensator (nc) equals the order of the plant. Unfortunately, these equations are highly coupled and are difficult to solve for the case $nc < n$. An alternative approach is to use a canonical structure to define the compensator,[13,14] which gives a minimal compensator parameterization and a simpler form for the necessary conditions.

Methods for improving the robustness of fixed-order dynamic compensator designs have been addressed in Ref. 7 and Refs. 14-16. Reference 14 uses a multimodeling approach to reduce sensitivity to parameter uncertainty. In Ref. 15, an upper bound for an H_2 performance index is minimized, subject to an H_∞ constraint that provides a guaranteed measure of robustness to unstructured uncertainty. This work was later extended in Ref. 7 to include robustness to parameter uncertainty by employing a quadratic Lyapunov bound.[17] The tightness of the H_2 bound and the Lyapunov bounds used in these studies remains a topic of current research interest. In Ref. 16, an approach is introduced that approximately recovers the performance and the multivariable gain and phase margins of a full state feedback design at the plant input. However, there

Presented as Paper 89-3458 at the AIAA Guidance, Navigation, and Control Conference, Boston, MA, Aug. 14-16, 1989; received Jan. 25, 1990; revision received Jan. 23, 1991; accepted for publication March 13, 1991.

*Professor, School of Aerospace Engineering. Associate Fellow AIAA.

†Graduate Research Assistant, School of Aerospace Engineering. Member AIAA.

is no guarantee that the closed-loop system remains stable in the presence of structured parameter uncertainty.

Outline

The main contribution of this paper is a simple formulation for designing fixed-order dynamic compensators that are robust to both unstructured uncertainty at the plant input and structured uncertainty in the plant dynamics. Specifically, the design method in Ref. 16 is extended to include a penalty on the trajectory sensitivity dynamics. The formulation avoids introducing the sensitivity states so that the overall problem dimension is not increased. The result is a quadratic weight selection that achieves parameter sensitivity reduction with minimal sacrifice in the loop transfer characteristics. Moreover, it is shown that by using an observer canonical form to define the compensator dynamics, the necessary conditions for optimality can be solved using a convergent algorithm for solving an equivalent constant gain output feedback problem.[18]

A brief outline of the paper follows. First the approximate recovery design technique of Ref. 16 for fixed-order dynamic compensation is reviewed. The main approach is then presented for reducing sensitivity to structured parameter uncertainty. The paper concludes with two design examples. The first example is used for comparison to a modified recovery approach for full order observer design.[19] The second example illustrates a realistic design of a yaw axis controller for a flexible satellite.

Approximate Loop Transfer Recovery at the Plant Input

In Ref. 16, an approximate loop transfer recovery (LTR) method is presented for designing fixed-order dynamic compensators by recovery of the loop properties of a full state controller at the plant input. This formulation is based on a performance index that penalizes the difference between two closed-loop return signals, corresponding to v_1 and v_2 in Fig. 1. These signals are produced by uniformly distributed impulses injected at the plant input for zero initial conditions. The details of this procedure are reviewed below.

Consider the standard linear multivariable system

$$\dot{x} = Ax + Bu, \qquad x \epsilon \Re^n,\ u \epsilon \Re^m \tag{1}$$

$$y = Cx + Du, \qquad y \epsilon \Re^p \tag{2}$$

which has the transfer function from u to y

$$G(s) = C\Phi B + D, \qquad \Phi = (sI - A)^{-1} \tag{3}$$

A compensator in observer canonical form[13] for the system in Eqs. (1) and (2) can be described as

$$\dot{z} = P^o_{ob} z + u_o, \qquad z \epsilon \Re^{nc} \tag{4}$$

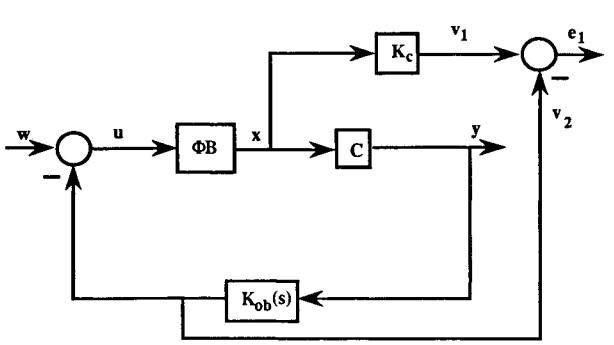

Fig. 1 Approximate LTR formulation for recovery at the plant input.

$$u_o = P_{ob} u - Ny, \qquad u_o \epsilon \Re^{nc} \tag{5}$$

$$u = -H^o z \tag{6}$$

where P_{ob} and N are free parameter matrices of compatible dimensions, and u_o is a fictitious control used in designing the compensator. The matrices P^o_{ob} and H^o are predetermined by the choice of observability indices v_i, and their structure is given below:

$$P^o_{ob} = \text{block diag } [P^o_1, \ldots, P^o_m] \tag{7}$$

$$P^o_i = \begin{bmatrix} 0 & 0 & & 0 & 0 \\ 1 & 0 & \ldots & 0 & 0 \\ 0 & 0 & & 0 & 0 \\ & & \vdots & & \\ 0 & 0 & \ldots & 0 & 0 \\ 0 & 0 & & 1 & 0 \end{bmatrix}_{v_i \times v_i} \tag{8}$$

$$H^o = \text{block diag } \{[0, \ldots, 0\ 1]_{1 \times v_i}, i = 1, \ldots, m\} \tag{9}$$

The observability indices are subject to the following constraints:

$$\sum_{i=1}^{m} v_i = nc, \qquad v_i \leq v_{i+1} \tag{10}$$

The compensator transfer function is given by Eq. (11):

$$K_{ob}(s) = H^o(sI - P^o_{ob} - P_{ob} H^o)^{-1} N \tag{11}$$

To formulate the previous equations as a constant gain output feedback problem, the system in Eqs. (1) and (2) is augmented with the observer canonical compensator, Eqs. (4-6), as defined in the following:

$$\dot{\boldsymbol{x}} = \boldsymbol{A}\boldsymbol{x} + \boldsymbol{B}u_o, \qquad \boldsymbol{x} \epsilon \Re^{n+nc} \tag{12}$$

$$\boldsymbol{y} = \boldsymbol{C}\boldsymbol{x}, \qquad \boldsymbol{y} \epsilon \Re^{p+m} \tag{13}$$

$$\boldsymbol{u} = -\boldsymbol{G}\boldsymbol{y} \tag{14}$$

where $\boldsymbol{x}^T = \{x^T, z^T\}$, $\boldsymbol{y}^T = \{y^T, -u^T\}$, and

$$\boldsymbol{A} = \begin{bmatrix} A & -BH^o \\ 0 & P^o_{ob} \end{bmatrix}, \qquad \boldsymbol{B} = \begin{bmatrix} 0 \\ I_{nc} \end{bmatrix} \tag{15}$$

$$\boldsymbol{C} = \begin{bmatrix} C & -DH^o \\ 0 & H^o \end{bmatrix}, \qquad \boldsymbol{G} = [N \quad P_{ob}] \tag{16}$$

The error signal to be penalized is given by

$$e_{ob} = v_1 - v_2 = K_c x - H^o z \tag{17}$$

where the full state gain K_c is designed for desirable loop properties at the plant input. The optimal linear quadratic regulator (LQR) full state design is usually chosen since it has guaranteed robustness properties at the plant input. However, in general, any stabilizing constant gain matrix may be used.

The approximate LTR performance index is

$$J = E_{x_o}\left\{\int_o^\infty [e^T_{ob} e_{ob} + \rho u_o^T u_o]\, dt\right\} \tag{18}$$

Substituting Eq. (17) into Eq. (18) and rewriting the performance index as

$$J = E_{x_o}\left\{\int_o^\infty [x^T Q x + u_o^T R u_o] dt\right\} \tag{19}$$

yields the following plant and compensator state weighting matrices:

$$Q = \begin{bmatrix} K_c^T K_c & -K_c^T H^o \\ -H^{oT} K_c & H^{oT} H^o \end{bmatrix}, \qquad R = \rho I_{nc} \tag{20}$$

By injecting uniformly distributed impulses at the plant input, the following initial condition variance is produced:

$$E\{x_o x_o^T\} = X_o = \begin{bmatrix} BB^T & 0 \\ 0 & 0 \end{bmatrix} \tag{21}$$

Equations (12–14) and (19) constitute a constant gain output feedback problem whose necessary conditions for optimality are well known.[20] As the parameter $\rho \to 0$, then $K_{ob}G$ approximates $K_c \Phi B$ to varying degrees depending on the order of the compensator. Although the full state loop transfer properties are recovered as ρ is reduced, the controller design may be sensitive to parameter uncertainty.

Reduction in Sensitivity to Uncertain Parameters

In this section, the approximate LTR formulation is extended to include a penalty on uncertain system parameters. First, a single scalar uncertainty parameter is introduced into the state equation, and then the trajectory sensitivity dynamics are developed. Next, the single scalar uncertainty parameter is included in the state and output equation and the necessary conditions for optimality are developed. Finally, the design equations are generalized to account for a vector of uncertain parameters in both the state and output equations.

Uncertain State Equation

Consider the system in Eqs. (1) and (2) with a single scalar uncertain parameter α in the state equation:

$$\dot{x} = A(\alpha)x + B(\alpha)u \tag{22}$$

Equation (12) becomes

$$\dot{x} = \boldsymbol{A}(\alpha)\boldsymbol{x} + \boldsymbol{B}\boldsymbol{u} \tag{23}$$

where

$$\boldsymbol{A}(\alpha) = \begin{bmatrix} A(\alpha) & -B(\alpha)H^o \\ 0 & P_{ob}^o \end{bmatrix}, \qquad \boldsymbol{B} = \begin{bmatrix} 0 \\ I_{nc} \end{bmatrix} \tag{24}$$

The trajectory sensitivity dynamics are obtained by differentiating the closed-loop system, Eqs. (23), (13), and (14), with respect to α:

$$\dot{\sigma} = (\bar{\boldsymbol{A}} - \boldsymbol{B}\boldsymbol{G}\boldsymbol{C})\sigma + \boldsymbol{A}_\alpha \boldsymbol{x}, \qquad \sigma(0) = 0 \tag{25}$$

where $\sigma = \partial x/\partial\alpha$, $\boldsymbol{A}_\alpha = \partial \boldsymbol{A}(\alpha)/\partial\alpha\,|_{\bar{\alpha}}$, $\bar{\boldsymbol{A}} = \boldsymbol{A}(\bar{\alpha})$, and $\bar{\alpha}$ denotes the nominal value for α. The standard approach would consider minimizing the performance index

$$J = E_{x_o}\left\{\int_o^\infty [\boldsymbol{x}^T\boldsymbol{Q}\boldsymbol{x} + u_o^T R u_o + \sigma^T V \sigma]\, dt\right\} \tag{26}$$

where the weighting matrix V is used to penalize sensitivity to parameter uncertainty. However, this increases the dimension of the optimization problem to $2(n+nc)$. To avoid this increase in dimension, the following viewpoint is adopted. Note that $\boldsymbol{A}_\alpha \boldsymbol{x}$ acts as a forcing function in Eq. (25) and that $\sigma(0) = 0$. Also note that if $\boldsymbol{G}$ stabilizes the nominal augmented system, then the dynamics of $\sigma(t)$ are also stable. Thus, $\|\sigma\|$ can be reduced by penalizing $\|\boldsymbol{A}_\alpha \boldsymbol{x}\|$. This suggests that the approximate LTR performance index in Eq. (18) can be modified to introduce a penalty on sensitivity to parameter uncertainty by weighting the square of the two norm of the forcing term in Eq. (25). Working from Eq. (19), the performance index is

$$J_s = E_{x_o}\left\{\int_o^\infty [\boldsymbol{x}^T(\boldsymbol{Q} + \eta \boldsymbol{A}_\alpha^T \boldsymbol{A}_\alpha)\boldsymbol{x} + u_o^T R u_o]\, dt\right\} \tag{27}$$

which does not involve the sensitivity states. Thus, a portion of the modeling information contained in Eq. (25) is discarded in favor of a more simplified formulation. A similar approach has been adopted in earlier work to suppress control and observation spillover.[21]

A second design parameter, $\eta \geq 0$, has been introduced in Eq. (27) that can be used to penalize sensitivity to parameter variations without increasing the order of the dynamic system. Equations (12–14) and (27) with $\boldsymbol{A} = \bar{\boldsymbol{A}} = \boldsymbol{A}(\bar{\alpha})$ constitute a static optimal output feedback problem, whose necessary conditions for optimality are well known.[20] When $\boldsymbol{Q}$, R, and X_o are chosen in accordance with Eqs. (20) and (21), then increasing η permits a design tradeoff between desirable loop transfer properties (loop broken at the plant input) and parameter sensitivity reduction.

Uncertain State and Output Equations

Next consider the system in Eqs. (1) and (2) with a single scalar uncertainty parameter in both the state and output equation:

$$\dot{x} = A(\alpha)x + B(\alpha)u \tag{28}$$

$$y = C(\alpha)x + D(\alpha)u \tag{29}$$

The augmented system, Eqs. (12–14), is now defined as

$$\dot{\boldsymbol{x}} = \boldsymbol{A}(\alpha)\boldsymbol{x} + \boldsymbol{B}\boldsymbol{u} \tag{30}$$

$$\boldsymbol{y} = \boldsymbol{C}(\alpha)\boldsymbol{x} \tag{31}$$

$$\boldsymbol{u} = -\boldsymbol{G}\boldsymbol{y} \tag{32}$$

where

$$\boldsymbol{A}(\alpha) = \begin{bmatrix} A(\alpha) & -B(\alpha)H^o \\ 0 & P_{ob}^o \end{bmatrix}$$

$$\boldsymbol{C}(\alpha) = \begin{bmatrix} C(\alpha) & -D(\alpha)H^o \\ 0 & H^o \end{bmatrix} \tag{33}$$

The trajectory sensitivity dynamics now become

$$\dot{\sigma} = (\bar{\boldsymbol{A}} - \boldsymbol{B}\boldsymbol{G}\bar{\boldsymbol{C}})\sigma + (\boldsymbol{A}_\alpha - \boldsymbol{B}\boldsymbol{G}\boldsymbol{C}_\alpha)\boldsymbol{x}, \qquad \sigma(0) = 0 \tag{34}$$

where, in addition to the earlier definitions for $\boldsymbol{A}_\alpha$ and $\bar{\boldsymbol{A}}$, $\boldsymbol{C}_\alpha = \partial \boldsymbol{C}(\alpha)/\partial\alpha\,|_{\bar{\alpha}}$, $\bar{\boldsymbol{C}} = \boldsymbol{C}(\bar{\alpha})$. Regarding $(\boldsymbol{A}_\alpha - \boldsymbol{B}\boldsymbol{G}\boldsymbol{C}_\alpha)$ as a forcing function in Eq. (34), then Eq. (27) becomes

$$J_s = E_{x_o}\left\{\int_o^\infty [\boldsymbol{x}^T\boldsymbol{Q}\boldsymbol{x} + u_o^T R u_o]dt\right\} \tag{35}$$

with

$$\boldsymbol{Q} = \boldsymbol{Q} + \eta f^T f \tag{36}$$

$$f = \boldsymbol{A}_\alpha - \boldsymbol{B}\boldsymbol{G}\boldsymbol{C}_\alpha \tag{37}$$

It can be seen from Eqs. (36) and (37) that the quadratic penalty on the states in the performance index depends explicitly on the gain matrix $\boldsymbol{G}$. Thus, the standard necessary conditions for optimal output feedback[20] no longer apply.

Using the basic approach outlined in Ref. 20, the necessary conditions for the output feedback problem defined by Eqs.

(30-32) and (35) are derived as follows. The performance index in Eq. (35) satisfies

$$J = tr\{KX_o\} \tag{38}$$

where K is the solution to

$$A_c^T K + KA_c + AQ + C^T G^T RGC = 0 \tag{39}$$

$$A_c = \bar{A} - BG\bar{C} \tag{40}$$

Defining the Lagrangian as

$$\mathcal{L} = tr\{KX_o + (A_c^T K + KA_c + Q + C^T G^T RGC)L^T\} \tag{41}$$

then the necessary conditions for optimality, $\partial\mathcal{L}/\partial K = \partial\mathcal{L}/\partial L = \partial\mathcal{L}/\partial G = 0$, are

$$A_c L + LA_c^T + X_o = 0 \tag{42}$$

$$A_c^T K + KA_c + AQ + C^T G^T RGC = 0 \tag{43}$$

$$RG\bar{C}L\bar{C}^T + \eta B^T BGC_\alpha LC_\alpha^T - B^T KL\bar{C}^T - \eta B^T A_\alpha LC_\alpha^T = 0 \tag{44}$$

Note that in the general case a closed-form expression for G cannot be obtained from Eq. (44). However, in the special case where $R = \rho B^T B$, B and $\bar{C}$ full rank, then

$$G = (B^T B)^{-1} B^T [KL\bar{C}^T + \eta A_\alpha LC_\alpha^T](\rho\bar{C}L\bar{C}^T + \eta C_\alpha LC_\alpha^T)^{-1} \tag{45}$$

Furthermore, for the observer canonical form used to define the compensator structure, $B^T = [0 I_{nc}]$, and $(B^T B)^{-1}$ simplifies to I_{nc} in Eq. (45). In addition for the observer canonical form, $B^T A_\alpha = 0$ so that $\eta B^T A_\alpha LC^T = 0$. A closed-form expression for G is needed if a sequential algorithm[18] is used to numerically solve the necessary conditions in Eqs. (42), (43), and (45).

Vector Parameter Uncertainty

Consider the uncertain system in Eqs. (30-32) where α now represents a vector of uncertain parameters. For this case, define σ_i as $\sigma_i = \partial x/\partial\alpha_i$, $i = 1, \ldots, h$, where α_i are the uncertain parameters. A set of equations is needed to define the sensitivity to each individual uncertain parameter. The trajectory sensitivity equations are now

$$\dot{\sigma}_i = (\bar{A} - BG\bar{C})\sigma_i + (A_{\alpha_i} - BGC_{\alpha_i})x, \qquad \sigma_i(0) = 0 \tag{46}$$

The quadratic performance index can be extended to penalize a weighted sum of the square of the two norms for each forcing term in Eq. (46). The sensitivity reduction penalty is now of the form

$$Q = Q + \eta \sum_{i=1}^{h} \gamma_i f_i^T f_i \tag{47}$$

$$f_i = A_{\alpha_i} - BGC_{\alpha_i} \tag{48}$$

$$\gamma_i = \Delta\alpha_i/\bar{\alpha}_i, \qquad \bar{\alpha}_i \neq 0 \tag{49}$$

where $\Delta\alpha_i$ is the maximum of $|\alpha_i - \bar{\alpha}_i|$, and $\bar{\alpha}_i$ is the nominal value for α_i. This definition of γ_i weights the penalty on the uncertain parameters in proportion to its expected worst case variation. The range of uncertainty is generally known as a design specification.

With the definitions for the weighting penalties in Eqs. (20) and (47-49), only two parameters, ρ and η, need to be adjusted during the design process. The parameter ρ is used to control the approximate recovery of the loop transfer properties, whereas the parameter η is used to reduce sensitivity to uncertain parameters.

The necessary condition in Eq. (42) remains unchanged whereas the necessary condition in Eq. (43) is used with the definition of Q in Eqs. (47-49). It is easily shown that the closed-form expression for G in Eq. (45) is replaced by

$$G = (B^T B)^{-1} B^T \left[KL\bar{C}^T + \eta \sum_{i+1}^{h} \gamma_i A_{\alpha_i} LC_{\alpha_i}^T \right]$$

$$\times \left(\rho\bar{C}L\bar{C}^T + \eta \sum_{i=1}^{h} \gamma_i C_{\alpha_i} \mathcal{L} C_{\alpha_i}^T \right)^{-1} \tag{50}$$

Thus, the design procedure for the vector parameter uncertainty case is no more difficult that the scalar case, and a sequential algorithm[18] can still be used to solve the necessary conditions for optimality.

Design Examples

Example 1: Parameter Uncertainty in the Output Matrix

This example treats the problem presented in Refs. 19 and 22. The system dynamics are given by

$$\dot{x} = \begin{bmatrix} -1 & 0 & 0 \\ 0 & -2 & 0 \\ 0 & 0 & -3 \end{bmatrix} x + \begin{bmatrix} 1 \\ -2 \\ 1 \end{bmatrix} u \tag{51}$$

$$y = [3 + \epsilon \;\; 3 \;\; 3]\, x \tag{52}$$

The uncertainty in this system is represented by the scalar parameter ϵ. In Ref. 19, it is shown that although a full state design is insensitive to variation in ϵ, a traditional LTR design results in observer poles that are sensitive to the uncertain parameter. This sensitivity results from the fact that the parameter variation lies outside the range space of the input matrix B. If the design is to be insensitive to ϵ, then the full state performance and robustness properties are sacrificed. In fact, in the limit, the optimal solution is achieved without feedback.

In Ref. 22, the full state feedback gain is first computed using

$$Q = \bar{C}^T\bar{C}, \qquad R = 0.01 \tag{53}$$

where $\bar{C} = C(\epsilon = 0)$, which results in the following full state gain matrix:

$$K_c = [17.3 \quad 10.5 \quad 6.67] \tag{54}$$

The closed-loop poles are at $s = -4.52$ and $-2.26 \pm 2.87j$.

A second-order compensator is selected to recover the full state feedback robustness properties. Using the weighting matrices in Eqs. (20) and (21), two compensators are designed for $\rho = 1.0 \times 10^{-3}$ and 1.0×10^{-8}. In Fig. 2, the Bode plots of the loop transfer functions with the loop broken at the plant input are shown for the full state design and the two compensator designs. The approximate recovery procedure is demonstrated by this plot. Note that for the $\rho = 1.0 \times 10^{-8}$ design, the dynamic compensator has nearly recovered the margins of the full state design.

The parameter uncertainty is next introduced into the design. Since the uncertainty occurs in the output matrix, the necessary conditions for optimality are given by Eqs. (42-44), with $A_\alpha = 0$. Several compensators are designed for $\rho = 1.0 \times 10^{-8}$ by sweeping the design parameter η from 0.0 to 2.5. In Fig. 3, the closed-loop sensitivity is shown as the uncertain parameter ϵ is varied from $-1 \leq \epsilon \leq 1$. These plots clearly illustrate that as η is increased, the system becomes insensitive to the uncertain parameter. Note that as ϵ is decreased in the $\eta = 0$ design, the plant poles become unstable, which differs from the traditional LTR design in Ref. 19 where the observer poles become unstable with ϵ variations.

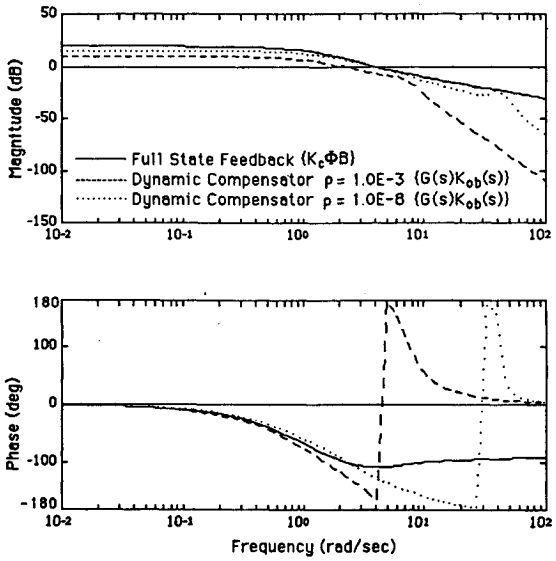

Fig. 2 Loop transfer functions for example 1.

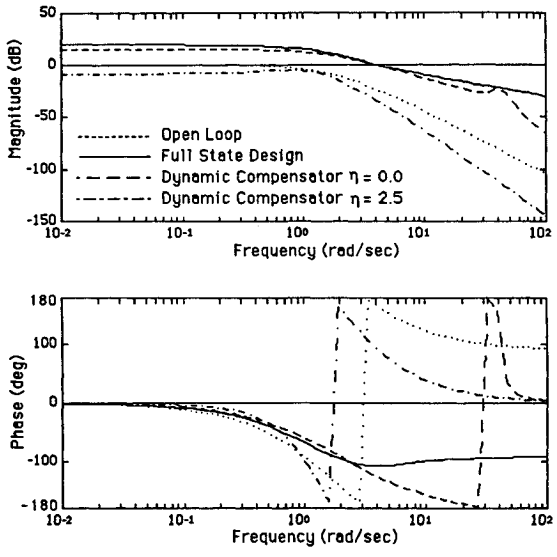

Fig. 4 Loop transfer functions for various η designs.

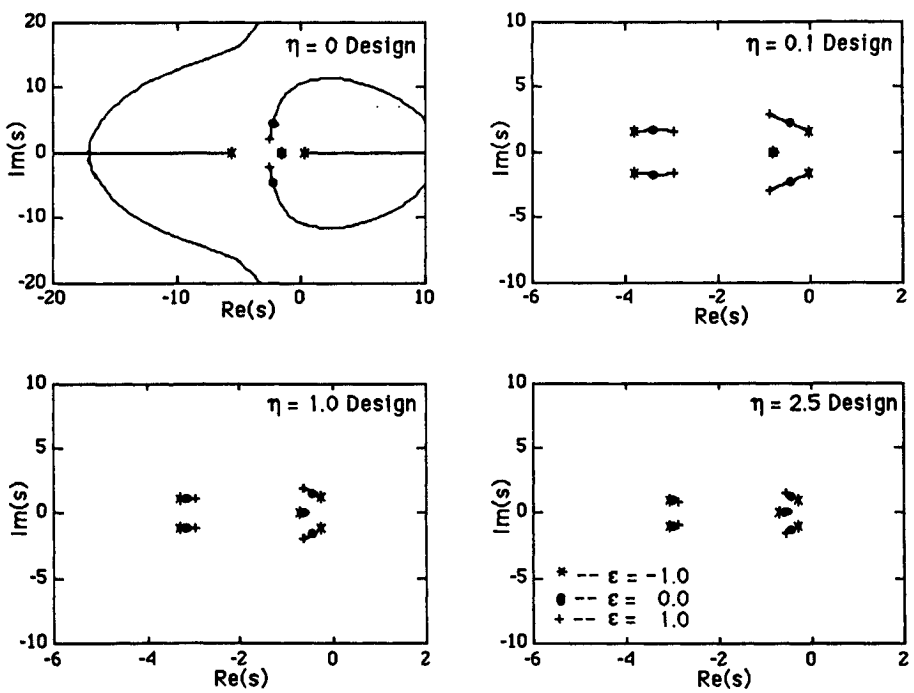

Fig. 3 Closed-loop poles vs ϵ for the $\rho = 1.0 \times 10^{-8}$ compensator design.

This difference is due to the fact that the separation principle is not applicable in fixed-order compensator design. Thus, the insensitivity of the full state design is not preserved.

As the parameter η is increased, the compensator designs are subject to a tradeoff between recovery of the full state loop properties and parameter sensitivity reduction. In Fig. 4, the magnitude of the loop transfer function with the loop broken at the plant input is shown for the parameter insensitive designs. As these plots clearly demonstrate, recovery is degraded as η increases and approaches the open-loop transfer function. It was found that the solution is essentially open-loop at $\eta \approx 5$, which agrees with the conclusion drawn for this example in Ref. 19.

Example 2: High Bandwidth Controller for a Flexible Spacecraft

This section illustrates the design of a robust attitude control system for a flexible spacecraft. In this problem, the actuators and sensors are collocated. Focusing on the yaw axis only, the model dynamics are

$$\mathfrak{M}\ddot{z} + \mathfrak{D}\dot{z} + \mathfrak{K}z = \mathfrak{B}u \tag{55}$$

where $z = \{\alpha, \delta\alpha\}^T$, $\mathfrak{B} = \{1, 0\}^T$, α is the yaw angle displacement in radians, $\delta\alpha$ is the modal displacement used to represent the flexible dynamics, and u is the control torque in inch-pounds. The coefficient matrices are

$$\mathfrak{M} = \begin{bmatrix} 77{,}511 & 248.1 \\ 248.1 & 1 \end{bmatrix}, \quad \mathfrak{D} = \begin{bmatrix} 0 & 0 \\ 0 & 0.002288 \end{bmatrix}$$

$$\mathfrak{K} = \begin{bmatrix} 0 & 0 \\ 0 & 0.098696 \end{bmatrix} \tag{56}$$

The equivalent first-order form is

$$\dot{x}_o = A_o x_o + B_o u \tag{57}$$

where $x_o = \{z^T \dot{z}^T\}^T$ and

$$A_o = \begin{bmatrix} 0 & I_2 \\ -\mathfrak{M}^{-1}\mathfrak{K} & -\mathfrak{M}^{-1}\mathfrak{D} \end{bmatrix}, \quad B_o = \begin{bmatrix} 0 \\ \mathfrak{M}^{-1}\mathfrak{B} \end{bmatrix} \tag{58}$$

This model was augmented to include the integral of α as a state variable, thus extending the controller design to a $P + I$ form. The introduction of the integral states insures good steady-state performance. Defining $x = \{z^T, \dot{z}^T, \int \alpha \, dt\}^T$, the linear model becomes

$$\dot{x} = Ax + Bu \tag{59}$$

where

$$A = \begin{bmatrix} A_o & \vdots & 0 \\ \cdots\cdots & + & \cdots \\ 1000 & \vdots & 0 \end{bmatrix} \tag{60}$$

The measured variables are taken as α, $\dot{\alpha}$, $\int \alpha \, dt$, and thus the output vector is defined as

$$y = Cx \tag{61}$$

with

$$C = \begin{bmatrix} 1 & 0 & 0 & 0 & 0 \\ 0 & 0 & 1 & 0 & 0 \\ 0 & 0 & 0 & 0 & 1 \end{bmatrix} \tag{62}$$

The purpose of the attitude control system is to maintain satellite pointing accuracy during a stationkeeping maneuver. The block diagram of the controller structure is shown in Fig. 5. The system specifications are 1) maintain a 0.02-deg pointing accuracy for a 1.0-in.-lbf step disturbance torque T_d at the plant input; 2) maintain this pointing accuracy in the presence on a 25% variation in structural frequency due to uncertainty in the stiffness matrix; and 3) provide at least $\pm$ 6 dB of gain margin and 40 deg of phase margin at the plant input for the nominal system.

These specifications require a controller bandwidth near the first flexible mode frequency, which is located at $\omega = 0.693$ rad/s. This makes sensitivity to uncertainty in the structural frequency a major design consideration. A classical design that relies on notch filtering would most likely fail to satisfy specification 2 above.

First a nominal LQR design is performed assuming full state feedback with

$$Q_{11} = 1, \qquad Q_{55} = 0.01, \qquad R = 10^{-7} \tag{63}$$

The weight Q_{55} is selected so as to avoid excessive settling times, and the control penalty R is selected so that the bandwidth of the control system is adequate. The resulting full state gain matrix is

$$K_c = [5058 \quad 11.0 \quad 24{,}640 \quad 64.87 \quad 316.2] \tag{64}$$

Figure 6 shows the Bode plot for this design obtained by breaking the loop at the plant input. Note that there is a downward gain margin of 15 dB, a phase margin of 60 deg, and a crossover frequency of $\omega_{cr} = 0.3$ rad/s.

Next, a third-order compensator is designed for the nominal system, using the weighting matrices in Eqs. (20) and (21), with the gain matrix K_c in Eq. (64). The necessary conditions in Eqs. (42), (43), and (45) were solved using the sequential algorithm in Ref. 18. The loop transfer Bode plots with the loop broken at the plant input for compensator designs of $\rho = 1.0$ and 0.01 are shown in Figs. 7 and 8, respectively. The effect of decreasing ρ clearly demonstrates that the loop transfer properties of the full state design can be successfully recovered with a third-order compensator. Note that the crossover frequency increases from $\omega_{cr} = 0.2$ rad/s to $\omega_{cr} = 0.25$ rad/s and that the downward gain margin increases from 10 to 13 dB as ρ is reduced. Moreover, the phase margin increases from 38 to 43 deg. Another interesting aspect is that for $\rho = 0.01$, the phase plot reaches a local maximum exactly at the crossover frequency. This desirable characteristic is not present in the $\rho = 1.0$ design Bode plot, and it is, in general, difficult to achieve using classical design methods. Comparison of Figs. 6 and 8 shows that the $\rho = 0.01$ design has nearly recovered the full state design loop transfer properties, but with a decrease in phase margin from 60 to 43 deg, which is considered acceptable. For the $\rho = 0.01$ design, the compensator free matrices are given below:

$$N = \begin{bmatrix} -2349 & -27{,}420 & -126.2 \\ 13{,}566 & 3853 & 173.4 \\ -18{,}971 & -48{,}036 & -613.8 \end{bmatrix}, \quad P_{ob} = \begin{bmatrix} 0.497 \\ 0.387 \\ 4.733 \end{bmatrix} \tag{65}$$

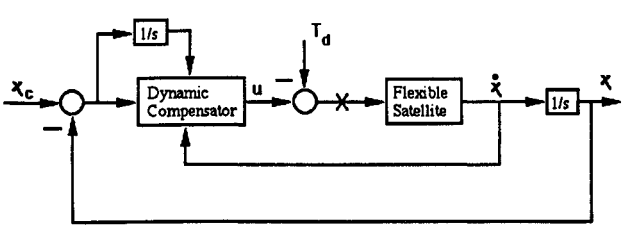

Fig. 5 Controller structure for example 2.

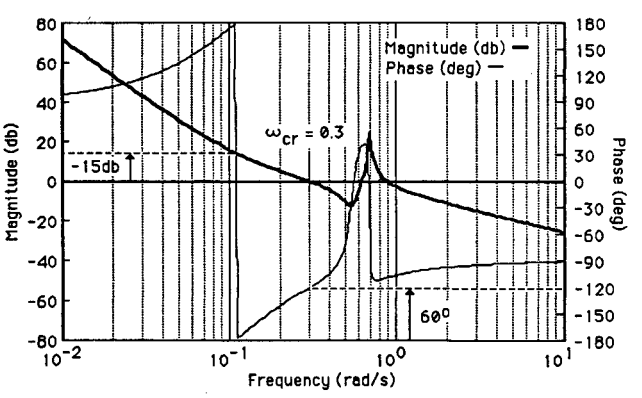

Fig. 6 Bode plot for the nominal full state feedback design.

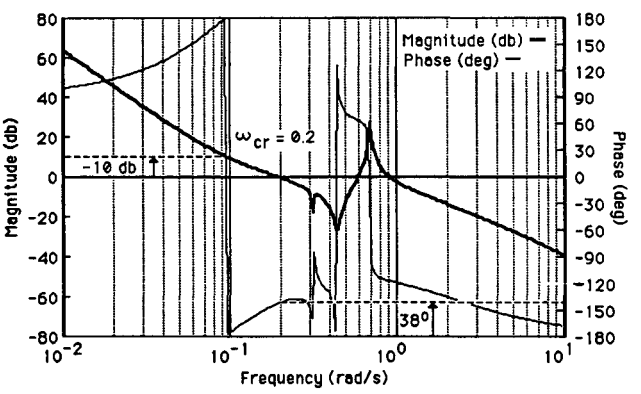

Fig. 7 Bode plot for dynamic compensator design with $\rho = 1.0$.

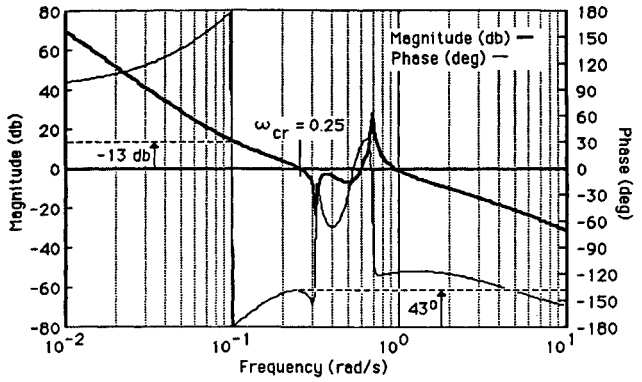

Fig. 8 Bode plot for dynamic compensator design with $\rho = 0.01$.

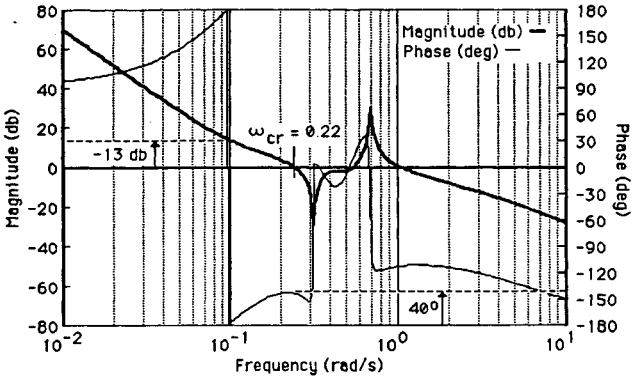

Fig. 10 Bode plot for dynamic compensator design with $\rho = 0.01$ and $\eta = 100$.

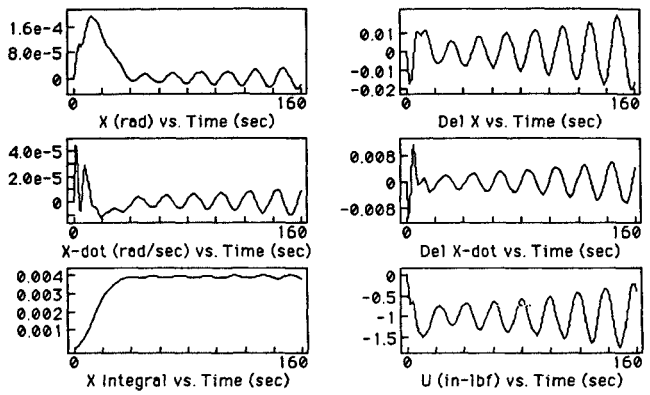

Fig. 9 Response of the dynamic compensator for $\beta = 0.22$.

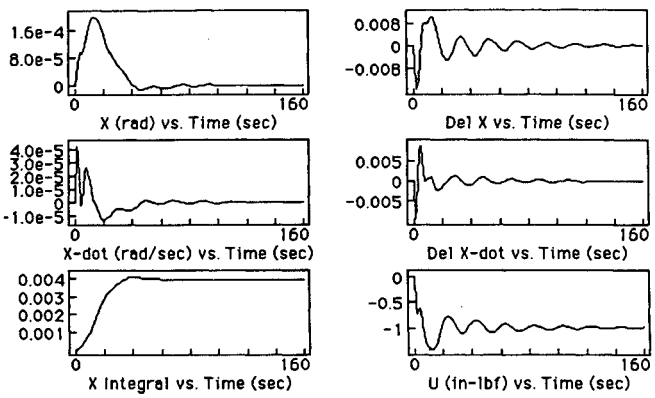

Fig. 11 Response of robust compensator for $\beta = 0.25$.

Sensitivity to parameter variations for this compensator design is investigated by evaluating the step disturbance with scalar uncertainty in the stiffness matrix of the form

$$\mathcal{K}_{\text{actual}} = (1 + \alpha)\mathcal{K} \tag{66}$$

In this case, $\alpha = 0.57$ corresponds to an increase in the structural mode natural frequency of approximately 25%, and $\alpha = -0.46$ results in a decrease of approximately 25%. In general, for $\mathfrak{M}$, $\mathfrak{D}$, and $\mathcal{K}$ diagonal, the fractional change in the structural mode frequency β is related to α by

$$\beta = (1 + \alpha)^{1/2} - 1 \tag{67}$$

Thus, the sensitivity results are parameterized by β in this example.

The controller described by the free parameter matrices in Eq. (65) is more sensitive to upward variation in β than to downward variation. This controller remains stable for a 25% decrease in the structural mode natural frequency. Therefore, only the results of the upward variations are presented. Figure 9 shows that the system becomes unstable when the structural mode natural frequency is increased by 22%. Thus, specification 2 is not satisfied.

Next, the performance index in Eq. (27) is used to penalize uncertainty of the form in Eq. (66). Figure 10 illustrates the Bode plot (loop broken at the plant input) that results from the design of a third-order compensator with $\rho = 0.01$ and $\eta = 100$. This should be compared with the Bode plot in Fig. 8. The downward gain margin has not changed from 13 dB. The phase margin has decreased slightly to 40 deg, and the crossover frequency is now $\omega_{cr} = 0.22$ rad/s. Thus, specification 3 is satisfied. Also, the phase plot maintains the local maximum at the crossover frequency. Note that the loop transfer functions are nearly the same for the two designs. However, there is a significant improvement in the closed-loop

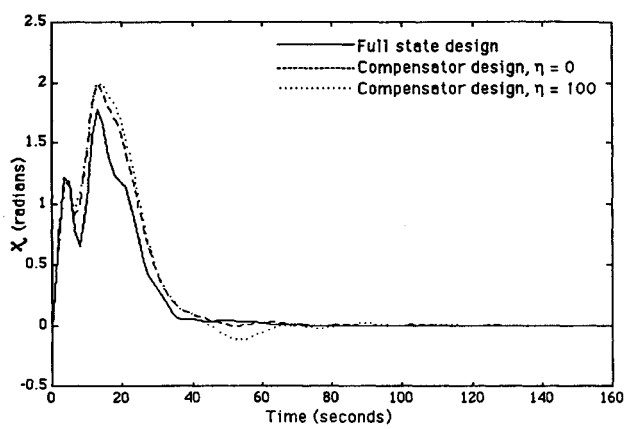

Fig. 12 Comparison of angular displacement due to a step disturbance.

system performance in the presence of the structured uncertainty, Fig. 11. Comparisons of Figs. 9 and 11 demonstrate that the instability for the $\eta = 0$ design has been removed in the $\eta = 100$ design. The closed-loop system remains stable beyond $\beta = 0.25$, and therefore the $\eta = 100$ design satisfied specification 2. For the $\rho = 0.01$, $\eta = 100$ design, the compensator free parameter matrices are given below:

$$N = \begin{bmatrix} -3146 & -30{,}090 & -183.8 \\ 6140 & 415.6 & 128.0 \\ -27{,}447 & -74{,}678 & -820.2 \end{bmatrix}, \quad P_{ob} = \begin{bmatrix} 0.718 \\ 1.118 \\ 6.078 \end{bmatrix} \tag{68}$$

Figures 12 and 13 summarize the time domain performance of the nominal system for the three designs: full state feed-

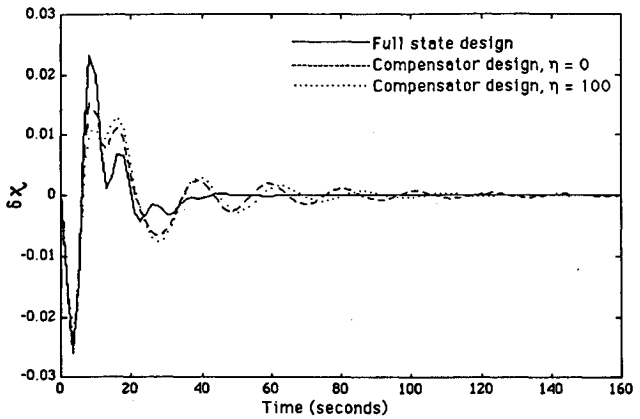

Fig. 13 Comparison of modal displacement due to a step disturbance.

back, dynamic compensation, and dynamic compensation with sensitivity reduction. In Fig. 12, a slight increase in peak yaw angular displacement occurs as the design progresses from full state feedback (0.0097 deg) to dynamic compensation with sensitivity reduction (0.0115 deg). All three designs satisfy specification 1. Figure 13 shows the comparison of modal displacement, where it is seen that the peak in modal response is reduced by dynamic compensation. The dynamic compensator with sensitivity reduction provides approximately 17% damping to the structure, which is a positive byproduct of this design.

Conclusions

A simple method of quadratic weight selection in fixed-order dynamic compensator design has been presented that permits a direct tradeoff between recovery of full state feedback loop properties and reduction in sensitivity to structured parameter variations. The approach is based on trajectory sensitivity reduction but does not require increasing the dimension of the optimization problem through the introduction of sensitivity states in the formulation. The tradeoff that results is highly problem dependent, as it would also be in other approaches. In example 1, reduced sensitivity is achieved only by reducing loop gain and thus sacrificing performance. The results in this example are directly comparable to a full order observer design based on a modified loop transfer recovery approach that reduces sensitivity to uncertain parameters. In example 2, it was possible to reduce sensitivity with little loss in loop transfer properties. The resulting controller satisfies all of the design requirements in terms of pointing accuracy, gain and phase margins, and robustness to variation in the structural frequency due to uncertainty in the stiffness matrix.

Acknowledgments

This research was supported by GE-Astro Space Division and by the Army Research Office under DAAL03-88-C-0003. The spacecraft example problem was formulated by Kidambi Raman of GE-Astro.

References

[1]Byun, K.-W., Wie, B., and Sunkel, J., "Robust Control Synthesis for Uncertain Dynamical Systems," AIAA Paper 89-3516, AIAA Guidance, Navigation, and Control Conference, Boston, MA, Aug. 1989.

[2]Byun, K.-W., Wie, B., Geller, D., and Sunkel, J., "New Robust H_∞ Control Design for the Space Station: Theory and Application," AIAA Paper 90-3319, AIAA Guidance, Navigation, and Control Conference, Portland, OR, Aug. 1990.

[3]Rhee, I., and Speyer, J. L., "A Game Theoretic Controller for a Linear Time-Invariant System with Parameter Uncertainty and Its Application to the Space Station," AIAA Paper 90-3320, AIAA Guidance, Navigation, and Control Conference, Portland, OR, Aug. 1990.

[4]Doyle, H. C., "Structured Uncertainty in Control System Design," IEEE Conference on Decision and Control, Fort Lauderdale, FL, Dec. 1985.

[5]Doyle, J. C., "Analysis of Feedback Systems with Structured Uncertainty," *Proceedings of IEEE*, Vol. 129, Pt. D, No. 6, Nov. 1982, pp. 242-250.

[6]Fan, M. K. H., Tits, A. L., and Doyle, J. C., "Robustness in the Presence of Joint Parametric Uncertainty and Unmodelled Dynamics," American Control Conference, Atlanta, GA, May 1988.

[7]Bernstein, D. S., and Haddad, W. M., "The Optimal Projection Equations with Petersen-Hollot Bounds: Robust Stability and Performance via Fixed Order Dynamics Compensation for Systems with Structured Real-Valued Parameter Uncertainty," *IEEE Transactions of Automatic Control*, Vol. AC-33, June 1988, pp. 578-582.

[8]Kriendler, E., "On the Definition and Application of the Sensitivity Function," *Journal of the Franklin Institute,* Vol. 285, No. 1, 1968, pp. 26-36.

[9]O'Reilly, J., "Low Sensitivity Feedback Controllers for Linear Systems with Incomplete State Information," *International Journal of Control*, Vol. 29, No. 6, 1979, pp. 1042-1058.

[10]Okada, K., and Skelton, R., "A Sensitivity Controller for Uncertain Systems," AIAA Paper 88-4077, AIAA Guidance, Navigation, and Control Conference, Minneapolis, MN, Aug. 1988.

[11]Johnson, T. L., and Athans, M., "On the Design of Optimal Constrained Dynamic Compensators for Linear Constant Systems," *IEEE Transactions on Automatic Control*, Vol. AC-15, No. 6, Dec. 1970, pp. 658-660.

[12]Hyland, D. C., and Bernstein, D. S., "The Optimal Projection Equations for Fixed Order Dynamic Compensation," *IEEE Transactions on Automatic Control*, Vol. AC-29, No. 11, Nov. 1984, pp. 1034-1037.

[13]Kramer, F. S., and Calise, A. J., "Fixed Order Dynamic Compensation for Multivariable Linear Systems," *Journal of Guidance, Control, and Dynamics,* Vol. 11, No. 1, 1988, pp. 80-85.

[14]Martin, G. D., and Bryson, A. E., "Attitude Control of a Flexible Spacecraft," *Journal of Guidance and Control*, Vol. 3, No. 1, 1980, pp. 37-41.

[15]Bernstein, D. S., and Haddad, W. M., "LQG Control with an H_∞ Performance Bound: A Riccati Equation Approach," *IEEE Transactions on Automatic Control,* Vol. AC-34, March 1989, pp. 293-305.

[16]Calise, A. J., and Prasad, J. V. R., "An Approximate Loop Transfer Recovery Method for Designing Fixed Order Compensators," *Journal of Guidance, Control, and Dynamics*, Vol. 13, No. 2, 1990, pp. 297-302.

[17]Petersen, I. R., and Hollot, C. V., "A Riccati Equation Approach to the Stabilization of Uncertain Systems," *Automatica*, Vol. 22, No. 4, 1986, pp. 397-411.

[18]Moerder, D. D., and Calise, A. J., "Convergence of a Numerical Algorithm for Calculating Optimal Output Feedback Gains," *IEEE Transactions on Automatic Control*, Vol. AC-30, Sept. 1985, pp. 900-903.

[19]Tahk, M., and Speyer, J. L., "Modeling of Parameter Variations and Asymptotic LQG Synthesis," *IEEE Transactions on Automatic Control*, Vol. AC-32, No. 9, Sept. 1987, pp. 793-801.

[20]Mendel, J. M., "A Concise Derivation of Optimal Constant Limited State Feedback Gains," *IEEE Transactions on Automatic Control*, Vol. AC-19, No. 4, Aug. 1974.

[21]Sesak, J. R., and Likins, D. D., "Model Error Sensitivity Suppression: Quasi-Static Optimal Control for Flexible Structures," IEEE Conference on Decision and Control, Fort Lauderdale, FL, Dec. 1988.

[22]Shaked, U., and Soroka, E., "On the Stability of the Continuous-Time LQG Optimal Control," *IEEE Transactions on Automatic Control*, Vol. AC-30, No. 10, Oct. 1985, pp. 1039-1043.